

LETTER


Fast tunable all-polarization-maintaining supercontinuum fiber laser for CARS microscopy

To cite this article: Kangwen Yang *et al* 2021 *Appl. Phys. Express* **14** 062004

View the [article online](#) for updates and enhancements.



Fast tunable all-polarization-maintaining supercontinuum fiber laser for CARS microscopy

Kangwen Yang¹ , Lizhong Huo¹, Jianpeng Ao², Qingting Wang¹, Qiang Hao¹, Ming Yan^{3,4}, Kun Huang^{3,4}, Minbiao Ji², and Heping Zeng^{1,3,4*}

¹Shanghai Key Laboratory of Modern Optical System, and Engineering Research Center of Optical Instrument and System, Ministry of Education, School of Optical Electrical and Computer Engineering, University of Shanghai for Science and Technology, Shanghai 200093, People's Republic of China

²State Key Laboratory of Surface Physics and Department of Physics, Human Phenome Institute, Multiscale Research Institute of Complex Systems, Academy for Engineering and Technology, Key Laboratory of Micro and Nano Photonic Structures (Ministry of Education), Fudan University, Shanghai 200433, People's Republic of China

³State Key Laboratory of Precision Spectroscopy, East China Normal University, Shanghai 200062, People's Republic of China

⁴Chongqing Institute of East China Normal University, Chongqing 401121, People's Republic of China

*E-mail: hpzeng@phy.ecnu.edu.cn

Received April 25, 2021; revised May 10, 2021; accepted May 14, 2021; published online May 26, 2021

We have demonstrated a compact fiber laser with broad and fast wavelength tunability for coherent anti-Stokes Raman scattering (CARS) microscopy. Originated from an Er-doped fiber laser, the Stokes pulses can be tuned from 1015 to 1060 nm within 300 μ s from supercontinuum of a tapered high nonlinear fiber, while pump pulses at 790 nm were obtained by second harmonic generation. The two beams were then sent to microscopes for CARS detection of oil, ethanol and mouse ear samples. This fast and broadly tunable fiber laser in the all-polarization-maintaining architecture would be promising to implement rapid label-free histology in clinical translation. © 2021 The Japan Society of Applied Physics

Coherent anti-Stokes Raman scattering (CARS) spectroscopy has shown its growing importance in biology and medical sciences as a label-free, non-invasive, and chemically selective spectroscopic technique.^{1,2)} In order to distinguish various chemical compounds in biomedical samples, at least one of the exciting laser wavelengths should be tuned to match different vibrational energy levels.^{3,4)} Currently, the widely used solid state optical parametric oscillator (OPO) still relies on temperature or angle tuning of parametric conversion crystals to meet this requirement. However, this system itself is complex, bulky and sensitive to the environment, let alone the slow tuning speed of temperature or angle, thus limiting its applications in clinical translation.

As an alternative, fiber-based laser source provides a compact, low-cost and alignment-free solution for CARS.^{5–7)} The most direct wavelength tuning method is inserting optical filter inside the fiber oscillator.⁸⁾ The major potential risk for this intracavity wavelength tuning is losing mode-locking caused by cavity misalignment. Another tuning method can be attributed to optical delay control in various nonlinear frequency conversion process. For example, the optical cavity length of a fiber OPO can be changed to continuously tune the signal wavelength due to dispersion filtering effect in a fiber laser based on four wave mixing.^{9–12)} A composite method with fast Stokes wavelength tuning and precision pump delay adjustment was proposed recently in a soliton self-frequency shift-based fiber laser.¹³⁾ These methods mainly rely on the optical delay control, thus their speed is usually limited by the velocity of mechanical stage.

In order to reduce the risk of losing mode-locking and improve the tuning speed, fast optical filter employing scanning mirror was presented and used to select the narrow band seed pulse from a broadened spectrum.^{14,15)} This method has been used in actively synchronized Ti:sapphire and Yb-doped hybrid laser system as well as passively synchronized Er- and Yb-doped fiber lasers for nonlinear biomedical imaging.^{9,16,17)} With the usage of resonant

scanning mirror, the tuning speed can reach to 8 kHz.^{18,19)} However, using two independent laser oscillators increases the system complexity. Both the active and passive synchronization induce additional cavity length or amplitude modulation, which might reduce the mode-locking stability. Therefore, using only one laser oscillator to generate dual-color synchronized pulses with fast external-cavity wavelength tunability would greatly simplify the laser scheme and improve the operation stability.

In this letter, we demonstrated an all-polarization-maintaining fiber laser with broad tuning range and fast tuning speed for CARS. The system was based on an all-fiber Er-doped oscillator mode-locked by nonlinear amplifying loop mirror (NALM).^{20–22)} The output was divided into two parts: one was amplified and frequency doubled to 790 nm as pump; the other was amplified and coupled into a tapered high nonlinear fiber for supercontinuum generation. We have built a tunable optical filter equipped with a galvanometric scanner for fast spectral selection from 1015 to 1060 nm. The selected Stokes pulses were combined with the pump to detect mouse ear, oil and ethanol. CARS spectroscopy and imaging were obtained.^{23,24)}

The experimental setup is shown in Fig. 1. It contained four parts: the laser oscillator, the Stokes branch, the Pump branch and the CARS detection. The laser oscillator was a passively mode-locked Er-doped fiber laser based on NALM. The cavity consisted of a 50 cm linear section comprising a fiber reflection mirror and a circuit section comprising a 70 cm Er-doped gain fiber (LIEKKI, Er80), a wavelength division multiplexer and a phase shifter. A 1×2 coupler with a splitting ratio of 4:6 was used to connect the linear and circuit sections. Stable mode-locking could be self-started with a repetition rate of 63 MHz. Output pulses from the oscillator were divided into two parts and sent to the Stokes and Pump branch separately.

The Stokes branch was based on spectral filtering of a supercontinuum excited by femtosecond Er-doped pulses. Cascade fiber amplifiers were used to amplify the seed pulses (EDFA-1, EDFA-2). We used high nonlinear fiber with zero

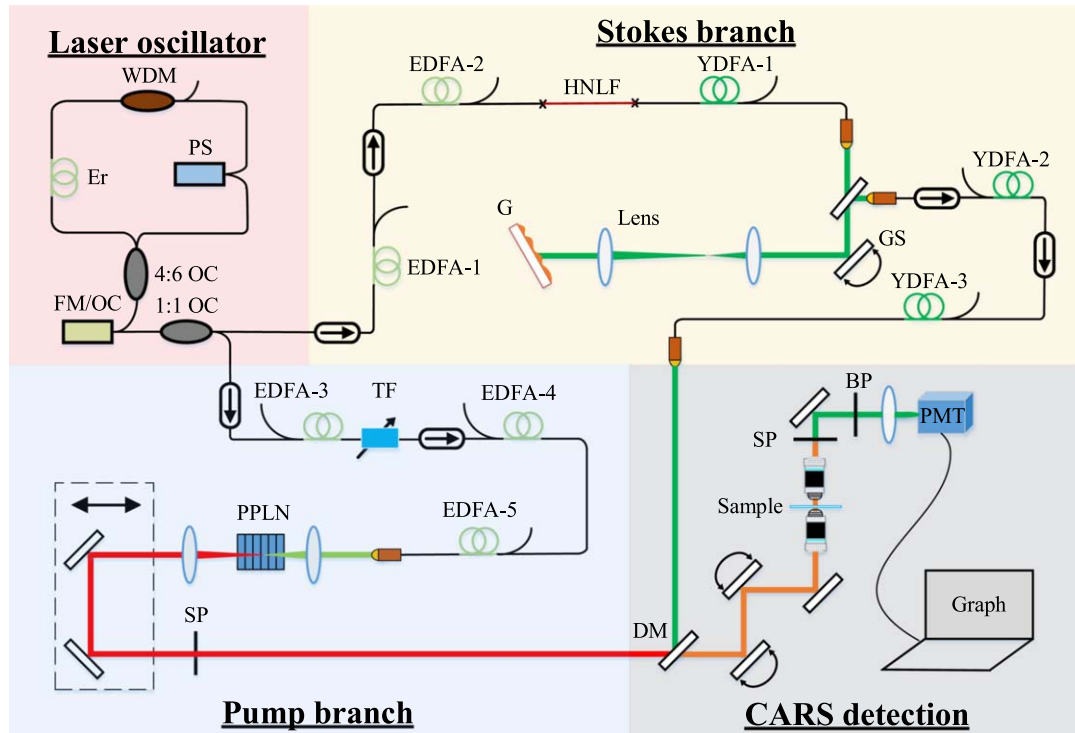


Fig. 1. (Color online) Experimental setup. WDM: wavelength division multiplexer; PS: phase shifter; FM: optical fiber mirror; OC: optical coupler; HNLF: high nonlinear fiber; G: grating; GS: galvanometer scanner; TF: tunable filter; SP: short pass filter; DM: dichroic mirror; BP: bandpass filter; PMT: photomultiplier tube.

dispersion wavelength at 1560 nm for spectral broadening. The generated supercontinuum was then used to seed a Yb-doped fiber amplifier (YDFA-1). By optimizing the splicing parameter, the splicing loss can be controlled down to 0.2 dB. Amplified pulses around 1030 nm are coupled to free-space and sent to a fast tunable optical filter with spectral bandwidth of 0.6 nm. It contains of a galvanometric scanner, a grating and a pair of lenses with focal length of 50 and 100 mm, respectively. By changing the reflection angle of the laser on the galvanometric scanner, rapid tuning of the laser wavelength can be achieved. The filtered pulses are then coupled into a two-stage Yb-doped fiber amplifier, which can provide narrowband Stokes laser.

The Pump branch was based on second harmonic generation (SHG) of spectral filtered Er-doped pulses. An Er-doped fiber pre-amplifier with gain fiber length of 1.5 m were used to broaden the spectrum (EDFA-3). Then we chose a commercially available optical filter with bandwidth of 1 nm to select the laser pulses. Cascaded Er-doped fiber amplifiers were used to boost the output power (EDFA-4, 5). The amplified pulses were then focused onto a PPLN with focal length of 30 cm. The period and length of the crystal is $20.2 \mu\text{m}$ and 20 mm, respectively. The PPLN crystal was placed in an oven whose temperature can be fine controlled from room temperature to nearly 400 K. Then frequency doubled pulses were collimated by a coated lens with 30 cm focal length. After that, a short pass filter with cut-off wavelength of 1000 nm was used to remove the fundamental frequency pulses.

Now we turn to characterize the supercontinuum generation from a tapered high nonlinear fiber. The output spectrum of our NALM oscillator was shown in Fig. 2(a). It had a central wavelength of 1569.4 nm and spectral bandwidth of

15.6 nm. The Kelly sidebands around the main peak indicates that the oscillator operates in the soliton region. After two-stage Er-doped fiber amplifiers, 66 fs laser pulses with average power of 170 mW were obtained before supercontinuum. The corresponding spectral bandwidth was 56.4 nm, as shown in Fig. 2(a).

Supercontinuum can be obtained by propagating energetic optical pulses through a piece of optical fiber. By using fiber taper technique, the reduced diameter of fiber core would induce very strong nonlinear interaction over a short length, thus outputting more broadband spectrum, as shown in Fig. 2(b). The HNLF used for tapering is a 10 cm long PM fiber with core effective area and nonlinear coefficient of $12.4 \mu\text{m}^2$ and $10.8 \text{W}^{-1} \text{km}^{-1}$. The central part of the HNLF was tapered by a CO_2 laser splicing system (LZM-100, AFL) with the fiber diameter down to $62 \mu\text{m}$, corresponding to a taper ratio of 2:1, as shown in Figs. 2(c) and 2(d). The laser intensity in the fiber core was increased by a factor of four within the tapered region. As a result, the leftmost wavelength of supercontinuum was extended from 1066 to 1000 nm. Although the current taper length was only 8 mm, the generated supercontinuum showed obvious broadening by fiber taper.

The generated supercontinuum provided laser pulses around $1.0 \mu\text{m}$, which were further amplified and sent to the tunable optical filter as the seed for Stokes. The filtered average power was about 0.3 mW with spectral bandwidth of 0.6 nm. A pre-amplifier with 1.5 m 6/125 gain fiber was used, outputting laser pulses of 3–20 mW with unchanged spectral bandwidth. Then a power amplifier consisting of 0.8 m 10/125 gain fiber was used to boost the output power. The average powers as well as spectra at different wavelengths were depicted in Fig. 3(a). The power curve for different

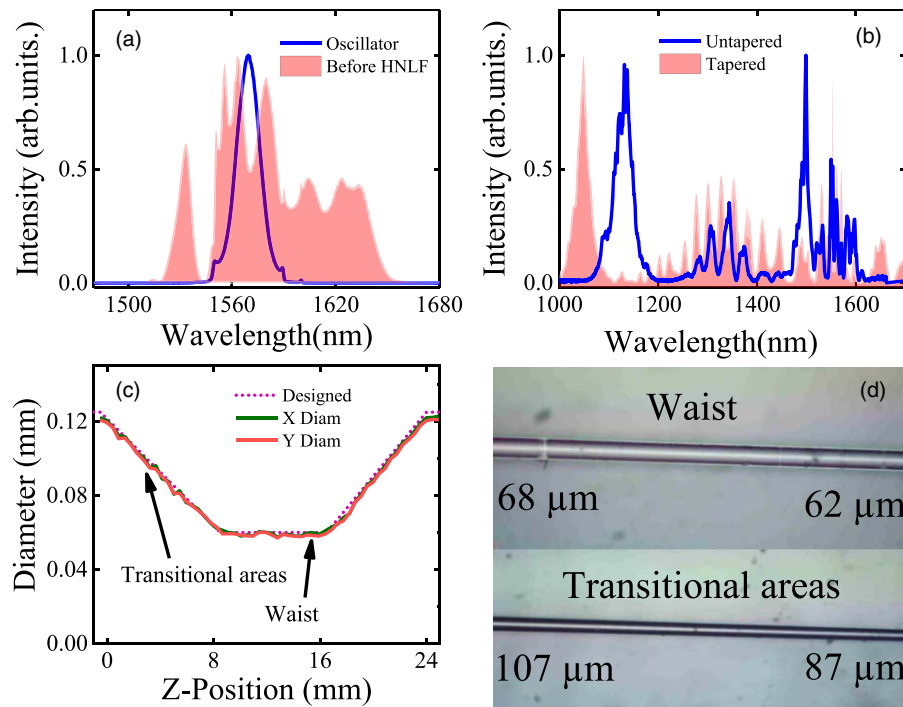


Fig. 2. (Color online) (a) Output spectra of the oscillator and amplifiers. (b) Supercontinuum from tapered and un-tapered HNLF. (c) Measured dimensions of the tapered region of the HNLF. (d) Microscope photos of the tapered HNLF in waist and transitional areas.

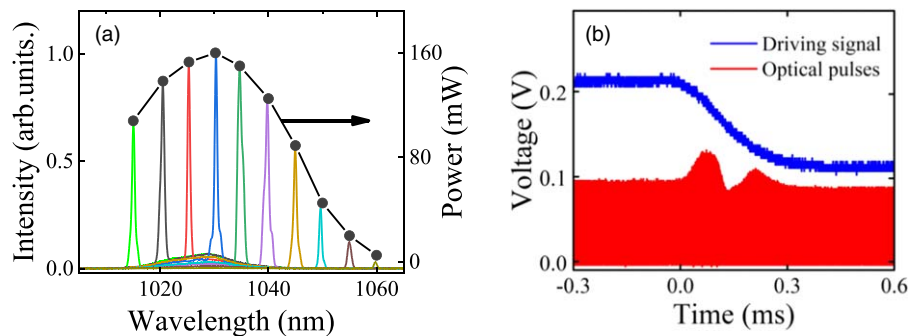


Fig. 3. (Color online) (a) Spectra and average powers at different wavelengths. (b) Oscilloscope traces of electrical driving signal and optical pulses when the wavelength was tuned from 1020 to 1030 nm.

wavelength was not flat, which is caused by the uneven emission cross section of the gain fiber. Although the average power in the longer wavelength range (larger than 1050 nm) was decreased dramatically, it should be noticed that the average power in wavelength range of 1020–1040 nm was larger than 120 mW, which is sufficient for covering the main peaks at frequently-used CH Raman bands (2850 cm^{-1} for CH_2 , 2930 cm^{-1} for CH_3). The spectral bandwidth was kept below 1.0 nm due to the usage of gain fiber with large core diameter.

Not only the average power and spectral bandwidth, but also the wavelength tuning speed of laser source were the important parameters for CARS application in biomedical area.²⁵⁾ To investigate the wavelength tuning speed, the scanner was driven by a rectangle wave at 50 Hz. Figure 3(b) shows the oscilloscope traces of driven signal directly applied to scanner and optical pulses measured when the wavelength was tuned from 1020 to 1030 nm. The measured wavelength tuning time was less than 300 μs , which was consistent with the temporal rising edge of the driven signal. The tuning speed was essentially determined

by the small step response of the scanner, which is about 300 μs in our case (TSH8203, Sunny Technology). By using fast galvanometer or resonant scanners (6210H or CRS series, Cambridge Technology), wavelength tuning time of less than 100 μs would be expected.²⁶⁾

In the following, we will characterize the output performance of Pump pulses, which were generated by frequency doubling of high-power narrow band Er-doped pulses. Seed pulses from Er-doped fiber oscillator were firstly amplified to 10 mW. Then a commercial tunable optical filter was used to select the central wavelength with bandwidth of 1 nm. The 2.0 mW selected pulses were then amplified to 100–200 mW by a power amplifier. The average power and corresponding spectra of tunable Er-doped pulses were shown in Fig. 4(a). The spectral bandwidths at different wavelengths varied from 0.7 to 1.7 nm due to the self-phase modulation and gain narrowing effects.

The amplified pulses were then used for SHG. The periods of PPLN crystal used in our experiment was 20.2 μm , corresponding to a phase matching wavelength of 1580 nm. As a result, we have fixed the central wavelength of Er-doped

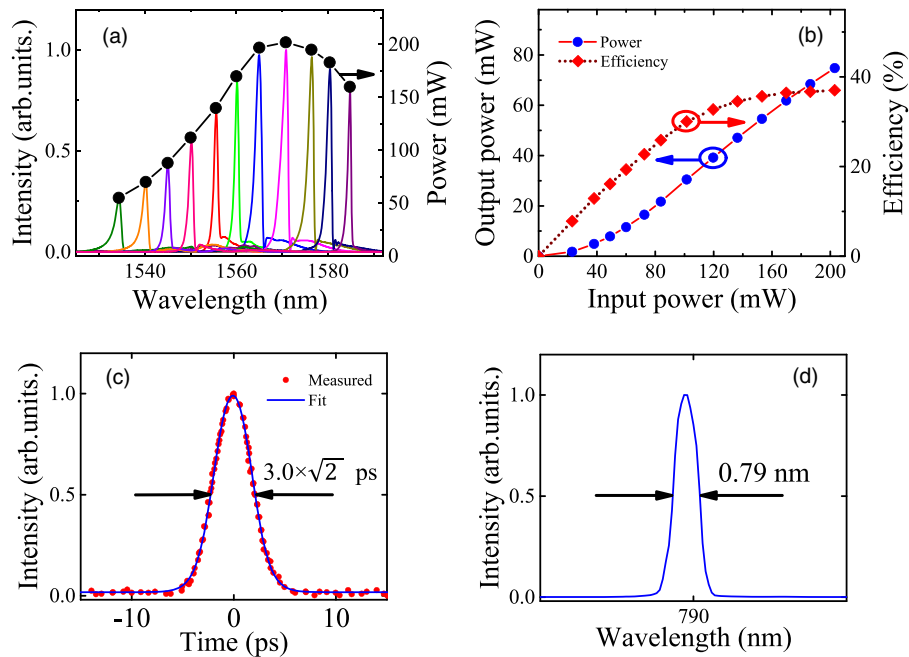


Fig. 4. (Color online) (a) The average powers as well as spectra at different wavelengths. (b) Output power and corresponding conversion efficiency for second harmonic generation. Autocorrelation trace (c) and spectrum (d) of second harmonic laser pulses.

laser to 1580 nm. In order to optimize the conversion efficiency, we changed the temperature of the crystal. It was found that the maximum output power of 75 mW can be achieved at 306 K, corresponding to a conversion efficiency of 37%, as shown in Fig. 4(b). At this power level, the temporal duration and spectral bandwidth were measured to be 3.0 ps and 0.79 nm, as shown in Figs. 4(c) and 4(d) respectively.

The Pump and Stokes laser were spatially combined by a dichroic mirror, their temporal overlap can be ensured by carefully tuning a free-space optical delay line. The combined dual-color laser pulses were firstly sent to a home-made microscope for obtaining CARS spectral signal. The microscope consisted of two identical microscope objectives with numerical aperture and magnification of 0.40 and 20. An optical short pass filter (700 nm) and a bandpass filter (640 ± 20 nm) were used to remove residual Pump and Stokes laser. A fiber coupled spectrometer (NIR 4000, Ocean Optics) with resolution of 3 nm was employed to record the CARS signal. We first perform CARS spectroscopy of ethanol and oil samples with Stokes pulses tuned from 1015 to 1055 nm, corresponding to Raman shift of $2806\text{--}3180\text{ cm}^{-1}$. The average powers for pump and Stokes pulses at the samples were 20 and 10 mW, respectively. As shown in Fig. 5(a), CARS signal at the Raman shifts of $2850\text{--}2960\text{ cm}^{-1}$ in olive oil and $2875, 2915, 2980\text{ cm}^{-1}$ in ethanol were clearly observed within the CH region, which agree with the results reported in previous publications.^{27,28)} Currently, the spectral resolution of CARS spectroscopy is limited by the spectrometer, which is about 37 cm^{-1} . Considering that the spectral bandwidth of pump pulse was 0.79 nm, CARS spectral resolution of 13 cm^{-1} would be expected. For nonlinear imaging, we coupled the Pump and Stokes laser pulses into a commercial microscope (Olympus, FV1200). The numerical aperture of the microscope objective was 1.2. The pixel dwell time was set to be $2\text{ }\mu\text{s}$. As a result, the imaging acquisition time for a 512×512 picture was

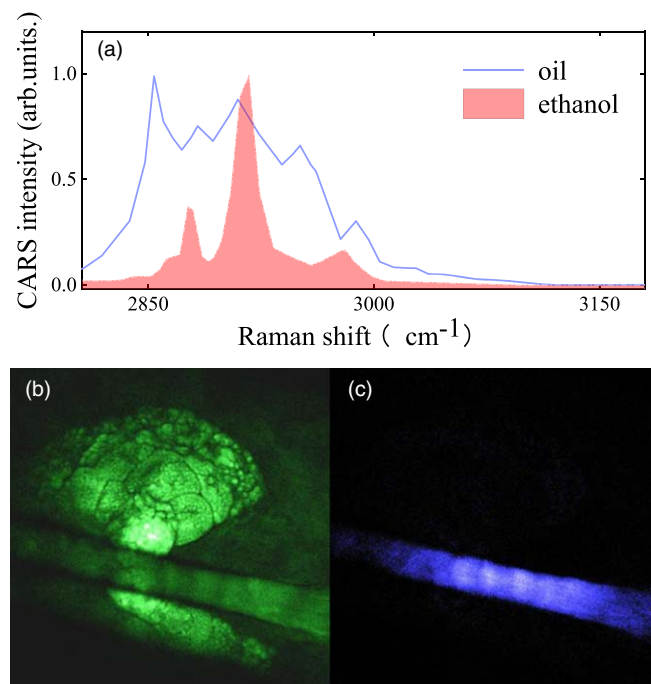


Fig. 5. (Color online) (a) Measured Raman spectra for olive oil and ethanol. (b) CARS and (c) SHG imaging of fresh mouse ear tissue.

1.08 s. CARS and SHG image can be obtained simultaneously by two-channel detection setup. As shown in Figs. 5(b) and 5(c), the CARS image at 2850 cm^{-1} indicates lipids distribution while the SHG represents the collagen distribution.

In summary, we have demonstrated a dual-color fiber laser source for CARS based on fiber amplification of spectrally filtered supercontinuum. The broad and fast wavelength tunability performance was made by the combination of tapering high nonlinear fiber and galvanometric scanner assisted optical filter. As a result, Stokes pulses from 1015 to 1060 nm can be tuned within $300\text{ }\mu\text{s}$, corresponding to

Raman shifts of 2806–3224 cm^{-1} . The presented laser source was used to excite olive oil, ethanol and mouse ear for spectroscopy and imaging, showing its applicability in substance identification and biomedical imaging. Thanks to the full polarization-maintaining fiber scheme, our fiber laser was immune to environmental perturbations such as mechanical vibration and temperature change. Moreover, the adopted artificial saturable absorber based on NALM as well as external-cavity wavelength tuning method ensure reliable self-starting behavior and eliminate risk of losing mode-locking. This stable, fast tunable dual-color fiber laser would accelerate the development of novel flow cytometry,²⁹⁾ disease diagnosis³⁰⁾ and material analysis.³¹⁾

Acknowledgments This work is supported by the National Natural Science Foundation of China (11974248, 61975033, 61875243), Science and Technology Innovation Program of Basic Science Foundation of Shanghai (18JC1412000), Shanghai Municipal Science and Technology Major Project (No. 2018SHZDZX01) and ZJLab, Program for Professor of Special Appointment (Eastern Scholar) at Shanghai Institutions of Higher Learning.

ORCID iDs Kangwen Yang  <https://orcid.org/0000-0001-7365-1793>

- 1) L. Wei, Z. Chen, L. Shi, R. Long, A. V. Anzalone, L. Zhang, F. Hu, R. Yuste, V. W. Cornish, and W. Min, *Nature* **544**, 465 (2017).
- 2) A. Virga, C. Ferrante, G. Batignani, D. De Fazio, A. D. G. Nunn, A. C. Ferrari, G. Cerullo, and T. Scopigno, *Nat. Commun.* **10**, 3658 (2019).
- 3) Y. Li, B. Shen, S. Li, Y. Zhao, J. Qu, and L. Liu, *Adv. Biol.* **5**, 2000184 (2021).
- 4) T. S. F. M. Heiko Linnenbank, *Adv. Photonics* **5**, 55001 (2019).
- 5) C. Zhang and J. Cheng, *APL Photonics* **3**, 90901 (2018).
- 6) C. W. Freudiger, W. Yang, G. R. Holtom, N. Peyghambarian, X. S. Xie, and K. Q. Kieu, *Nat. Photonics* **8**, 153 (2014).
- 7) D. A. Orringer et al., *Nat. Biomed. Eng.* **1**, 0027 (2017).
- 8) Y. Mashiko, E. Fujita, and M. Tokurakawa, *Opt. Express* **24**, 26515 (2016).
- 9) K. Yang, P. Ye, S. Zheng, J. Jiang, K. Huang, Q. Hao, and H. Zeng, *Opt. Express* **26**, 2995 (2018).
- 10) T. Gottschall, T. Meyer, M. Schmitt, J. Popp, J. Limpert, and A. Tünnermann, *Opt. Express* **23**, 23968 (2015).
- 11) K. Yang, J. Jiang, Z. Guo, Q. Hao, and H. Zeng, *IEEE Photonics Tech. Lett.* **30**, 607 (2018).
- 12) K. Yang, S. Zheng, Y. Wu, P. Ye, K. Huang, Q. Hao, and H. Zeng, *Opt. Express* **26**, 17519 (2018).
- 13) Y. Zhang, J. Jiang, K. Liu, S. Wang, Z. Ma, and T. Liu, *Appl. Phys. Express* **13**, 92002 (2020).
- 14) Y. Ozeki, W. Umemura, K. Sumimura, N. Nishizawa, K. Fukui, and K. Itoh, *Opt. Lett.* **37**, 431 (2012).
- 15) Y. Ozeki, W. Umemura, Y. Otsuka, S. Satoh, H. Hashimoto, K. Sumimura, N. Nishizawa, K. Fukui, and K. Itoh, *Nat. Photonics* **6**, 845 (2012).
- 16) Y. Ozeki, T. Asai, J. Shou, and H. Yoshimi, *IEEE J. Sel. Top. Quantum* **25**, 1 (2019).
- 17) K. Yang, Y. Shen, J. Ao, S. Zheng, Q. Hao, K. Huang, M. Ji, and H. Zeng, *Opt. Express* **28**, 13721 (2020).
- 18) M. Brinkmann, A. Fast, T. Hellwig, I. Pence, C. L. Evans, and C. Fallnich, *Biomed. Opt. Express* **10**, 4437 (2019).
- 19) S. Bégin, B. Burgoyne, V. Mercier, A. Villeneuve, R. Vallée, and D. Côté, *Biomed. Opt. Express* **2**, 1296 (2011).
- 20) N. Kuse, J. Jiang, C. C. Lee, T. R. Schibli, and M. E. Fermann, *Opt. Express* **24**, 3095 (2016).
- 21) T. Jiang, Y. Cui, P. Lu, C. Li, A. Wang, and Z. Zhang, *IEEE Photonics Tech. Lett.* **28**, 1786 (2016).
- 22) W. Hänsel et al., *Appl. Phys. B* **123**, 41 (2017).
- 23) M. Tani, T. Koizumi, H. Sumikura, M. Yamaguchi, K. Yamamoto, and M. Hangyo, *Appl. Phys. Express* **3**, 72401 (2010).
- 24) Y. Yang, L. Chen, and M. Ji, *J. Innov. Opt. Health Sci.* **10**, 1730010 (2017).
- 25) R. He, Y. Xu, L. Zhang, S. Ma, X. Wang, D. Ye, and M. Ji, *Optica* **4**, 44 (2017).
- 26) J. Shou and Y. Ozeki, *Appl. Phys. Lett.* **113**, 33701 (2018).
- 27) Y. Qin, B. Cromei, O. Batjargal, and K. Kieu, *Opt. Lett.* **46**, 146 (2021).
- 28) J. Yuan, G. Zhou, C. Xia, X. Sang, F. Li, C. Yu, K. Wang, B. Yan, H. Y. Tam, and P. K. A. Wai, *IEEE Photonics Tech. Lett.* **28**, 763 (2016).
- 29) Y. Suzuki et al., *Proc. Natl. Acad. Sci.* **116**, 15842 (2019).
- 30) B. Zhang, H. Xu, J. Chen, X. Zhu, Y. Xue, Y. Yang, J. Ao, Y. Hua, and M. Ji, *Theranostics* **7**, 3074 (2021).
- 31) J. Ao, Y. Feng, S. Wu, T. Wang, J. Ling, L. Zhang, and M. Ji, *Small Methods* **4**, 1900600 (2020).